International Conference on Space Optics—ICSO 2018

Chania, Greece

9–12 October 2018

Edited by Zoran Sodnik, Nikos Karafolas, and Bruno Cugny

Design and manufacture of 1.3 meter large caliber light-weighted Space optical components

Xiaoyong Wang

Chongling Guo

Yong Liu

Jiayi Chen

et al.

International Conference on Space Optics — ICSO 2018, edited by Zoran Sodnik, Nikos Karafolas, Bruno Cugny, Proc. of SPIE Vol. 11180, 111800S · © 2018 ESA and CNES · CCC code: 0277-786X/18/$18 · doi: 10.1117/12.2535947

Design and manufacture of 1.3 meter Large caliber Light-weighted Space Optical components

Wang xiaoyong[*a], Guo chongling[*a], Liu yong[*a], Chen jiayi[*a], Wang yonggang[*a], Hu yongli[*a]

[a]Beijing Institute of Space Mechanics and Electricity,104 YouYi Road, Haidian, Beijing, CHINA 100094

ABSTRACT

The large-caliber light-weight reflector assembly is the core optical component of the large-size space camera. It needs to be highly light-weight to meet the constraint of emission weight. At the same time, the on-orbit reflector assembly needs to have extremely high force and thermal stability, be able to withstand the changes in the in-orbit temperature environment and the resulting stress changes and maintain the profile quality. This paper introduces the development of 1.3m caliber space mirror module. The reflector adopts the uniform thickness back arc design and the positioning support adopts the six-bar Bipod support technology. The simulation analysis verifies that the reflector component has good force and heat stability. The optical axis vertical test is carried out on the surface of the reflector assembly which has been processed and adjusted. The test results are consistent with the mechanical analysis results of the reflector assembly under the condition of gravity field, which meets the technical requirements of the spatial reflector.

Keywords: Large caliber reflector, light weight, honeycomb core, Bipod support

1. INTRODUCTION

The large-caliber light-weight reflector assembly is the core optical component of the large-size space camera. It needs to be highly light-weight to meet the constraint of emission weight. At the same time, the on-orbit reflector assembly needs to have extremely high force and thermal stability, be able to withstand the changes in the in-orbit temperature environment and the resulting stress changes and maintain the profile quality. The high light weight mirror brings great difficulties to the optical processing and detection. The influence of gravity detected on the ground will also cause the mirror surface deformation, which makes it difficult to obtain the surface shape data under zero gravity. The high lightweight reflector has low stiffness and needs strong support, while too many supporting points make the reflector component extremely vulnerable to the impact of external environment changes, resulting in system instability. The solution of the above problems is very important to the development of large space camera.

This paper introduces the development of the 1.3m-caliber lightweight reflector assembly, which is a quadratic ellipsoid surface. The main technical requirements are shown in Table 1:

Table 1. Mirror technical requirements

The reflector's effective aperture D	φ1280mm
Mirror center hole d	φ300mm

Mirror vertex radius of curvature R	-3477.17±1mm
Mirror aspheric coefficient k	-0.9827
Mirror thickness	120mm~160mm
Mirror weight	< 90kg
Mirror zero gravity profile（RMS）	0.02 λ
External dimensions envelope of reflector assembly (including supporting structure)	< φ1300×390 mm
Weight of reflector assembly (including supporting structure)	< 115kg

This mirror requires a high degree of light and large aperture, and it is very difficult to process and detect the shape of the mirror. The supporting structure weight of the mirror is only 25kg, which meets the requirement of extremely high mechanical thermal performance and stability of the reflector assembly[1]. This paper analyzes and optimizes the design, processing, detection and assembly of ultra-light large-caliber mirror, solves the technical problems of high-precision surface machining, zero-gravity profile detection, high-stability static support, high-precision measurement and assembly, and solves the key technical problems of developing large-caliber light-duty camera.

2. LIGHTWEIGHT REFLECTOR DESIGN

The reflector assembly is a complex structure, and it is difficult to obtain the optimal performance of the mirror billet structure. Choosing effective lightweight structure and determining optimal structure parameters is the most practical and effective way to improve the lightweight degree of reflector based on existing materials and processes. The light weight structure reflector of honeycomb sandwich is higher than that of other light weight structure in the same stiffness and strength[2]. Therefore, 1.3m caliber reflector adopts the light weight structure of honeycomb sandwich and adopts the circular arc design of the back with equal thickness configuration. The light weight structure of the reflector is optimized on the basis of determining the configuration.

The sandwich structure of the mirror consists of a base plate, a reflector and a sandwich layer. The structure performance of the mirror is mainly determined by the thickness of the reflector, the thickness of the bottom plate and the sandwich layer.

The thickness of the reflector plate affects the rigidity of the whole structure of the mirror[3]. When the thickness of the reflective panel is too large, the overall mass of the mirror increases and the specific stiffness decreases. The thickness of the reflective panel is too small, and the requirement of the mirror blank is too high. The bottom plate forms the closed structure of the mirror and enhances the rigidity of the structure.

Sandwich layer is the main contributor to the high specific stiffness of mirror. Common structural forms of sandwich layer include triangular structure, square structure, hexagon structure and fan-shaped structure (see Figure 1). The four structures are superior in weight, structural rigidity and ease of fabrication.

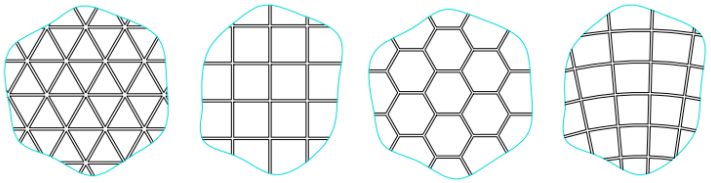

Figure 1. Honeycomb grid structure

The structural parameters of sandwich layer mainly include: thickness of outer ring, shape and thickness of inner ring, thickness of grid plate and length of grid plate. Respectively, square sandwich structure of hexagonal sandwich structure, sandwich structure and sandwich structure triangle sector a lot of detailed simulation optimization and comparison analysis, finally Φ 1300 mm sandwich reflector adopts the structure of the project is shown in Figure 2 and shown in Table 2.

Table 2. 1300 mm Φ sandwich reflector optimization of structure parameters

Diameter	Honeycomb length of side	Case thickness	Panel thickness	The back thickness	The ring thickness	The lateral high	The back of the curvature	weight
1300mm	30mm	3.5-5.5mm	9mm	7mm	5mm	120mm	SR3509.9mm	90kg

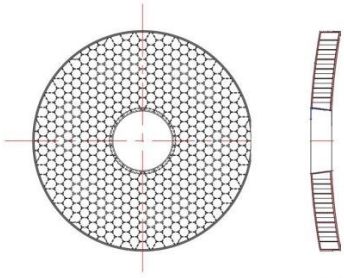

Figure 2. Φ 1300 mm sandwich lightweight mirror structure

Finite element analysis was carried out on the reflector scheme, and detailed mesh division was conducted on the geometric model using the preprocessing software, as shown in figure 3. Both grid density and cell quality can meet the requirement of accuracy of simulation calculation.

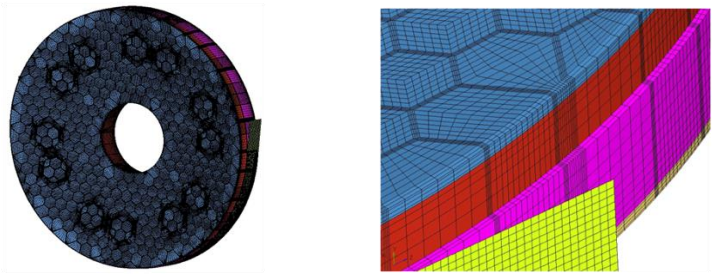

Figure 3. finite element model of reflector

2.1. Mechanical analysis

Under the free boundary condition of the mirror, the first ten second order modes of the mirror are calculated, and the first order non-zero mode frequency is required to be no less than 360Hz. The

results of the free modal analysis of the reflector are calculated, as shown in Table 3. The results show that the first order non-zero frequency is 414Hz, which meets the design requirements. Figure 4 shows the modal patterns of 7 to 12.

Table 3. Free vibration frequency of mirror

Number	frequency（Hz）
1~6	0
7	414.19
8	414.19
9	691.31
10	946.27
11	962.29
12	1098.16

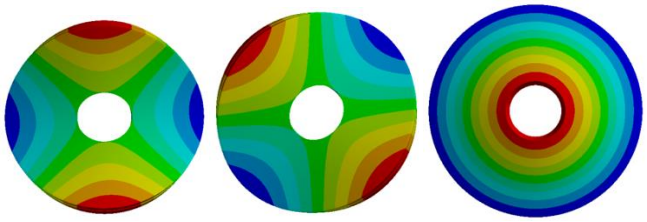

Figure 4. free vibration mode

2.2. Temperature deformation analysis

Simulation analysis under the condition of uniform temperature rise of 2 degrees mirror free state surface shape accuracy drops, result should satisfy the surface shape accuracy is not greater than the □/ 250 request, computing simulation results are shown in Figure5. The results showed that RMS=0.002nm after the lens face shape was removed and the defocusing surface shape RMS=0.83nm after the temperature rose by 2 degrees. Meet the design requirements.

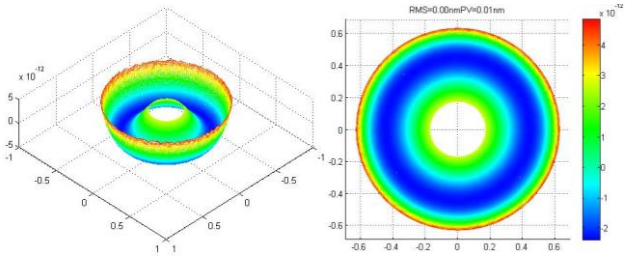

(a) remove defocusing

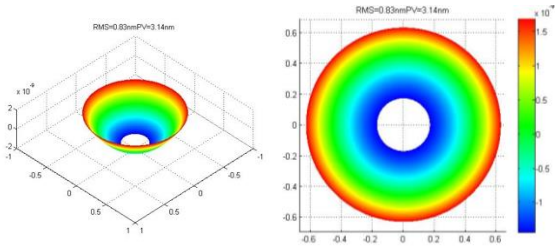

(b) do not remove defocusing

Figure 5. surface shape with temperature rising 2 degrees

2.3. Analysis of gravity deformation in the vertical state of the optical axis

When analyzing the self-weight deformation in the vertical state of the optical axis, the degrees of freedom of all nodes in the support area of the back of the constraint reflector in the direction of the optical axis. Meanwhile, in order to ensure that the rigid body displacement does not occur in the calculation process, select one node in the support area and select three translational degrees of freedom of constraint. The reflector back USES 60 back support points, as shown in figure 10.

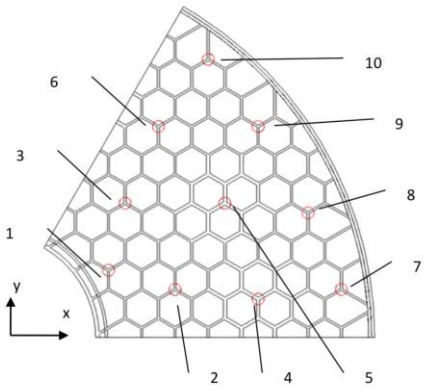

Figure 6. support distribution at 60 points on the back of the reflector

The coordinates of the center of the support region and the support force obtained by the optimization calculation are shown in table 4, where only one of the six symmetric support points is listed. The coordinate direction is based on the X and Y coordinates in figure 6. In the whole mirror calculation model, the horizontal friction force is about 4 orders of magnitude lower than the axial support force.

Table 4. Axis vertical back support point coordinates and support force

number	Coordinate values /mm	support force /N	number	Coordinate values /mm	support force /N
1	（194.12，112.07）	12.2	6	（277.31.352.23）	12.3
2	（305.04，80.05）	11.9	7	（582.35，80.05）	13.7
3	（221.85，224.15）	12.0	8	（526.88，208.13）	14.4
4	（443.69，64.04）	16.8	9	（443.69，352.23）	14.4
5	（388.23，224.15）	17.4	10	（360.50，464.30）	13.8

When the support diameter respectively take Φ 20 mm, Φ 25 mm and Φ 30 mm, reflective surface gravity deformation nephogram as shown in figure 7, reflective surface gravity deformation of RMS are shown in table 5, the results show that the back 60 points gravity discharge indexes meet the design requirements.

Table 5. Optical axis vertical unloading reflection face RMS

Diameter of support area	20mm	25mm	30mm
The form RMS/nm	2.73	2.59	2.46

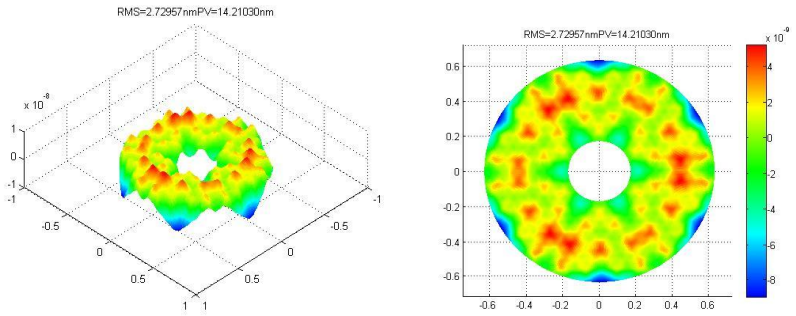

(a) Φ 20 mm support condition of mirror surface

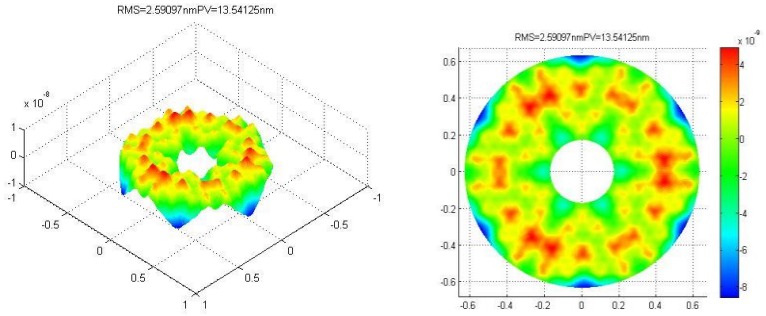

(b) Φ 25 mm support condition of mirror surface

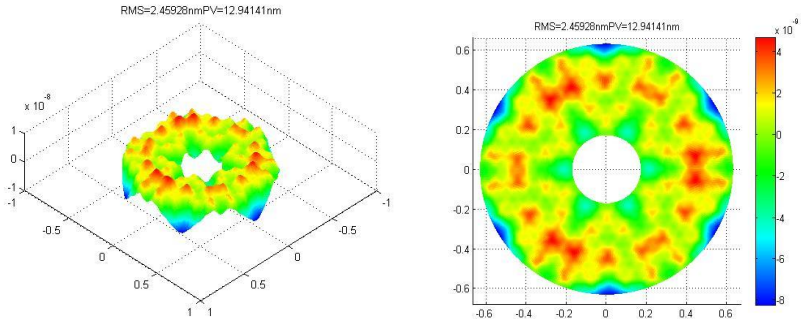

(c) Φ 30 mm support condition of mirror surface

Figure 7. vertical multi-point unloading surface shape of optical axis

Sensitivity analysis was carried out on the support reaction force, calculation 1 n force opposite form as a result, the influence of corresponding Φ 30 mm support as a result, the increase of support at no. 1,2,4,7 reaction respectively, its surface shape changes as shown in table 6. The maximum value of planar RMS is 2.94nm, indicating that the change of 1N force affects about 0.5nm.

Table 6. Surface shape under the action of 1N

Number	1	2	4	7
RMS/nm	2.51	2.72	2.94	2.89

Through the above design and analysis, the reflector has a good thermal performance, and the gravity discharge can be achieved by adopting 60 points of support under the vertical optical axis, which is conducive to the detection and assembly adjustment of the reflector.

3. MIRROR SUPPORTING STRUCTURE DESIGN

Large-diameter primary mirror supporting technology has been one of the key technology of space camera is developed, on the one hand mirror support system must ensure that the launch is not destroyed in the process, which requires the support structure has high enough dynamic stiffness and strength, on the other hand mirror system must make the pledge that we shall have a high enough position in space orbit environment precision and accuracy, which requires the mirror system has a high enough thermal stability[4]. However, these two aspects are often contradictory, and the design is to seek a good compromise in this contradiction, so that the reflector system meets both the stiffness and strength requirements and the dimensional thermal stability requirements. Kinematics support is an ideal form to meet the requirements of mirror support. However, it is difficult to realize in reality. The quasi-kinematics supporting mode can effectively isolate the influence of external factors on the reflector, including the influence of stress in the assembly process and environmental changes. It has been widely used in practical design. 1.3m-calibre mirror positioning support adopts the six-bar Bipod static and fixed support mode that conforms to kinematic support. The whole reflector assembly is composed of reflector, invar pad, Bipod bar, thermal compensation cylinder and base connected with the main bearing plate. The model of reflector assembly is shown in figure 8 below:

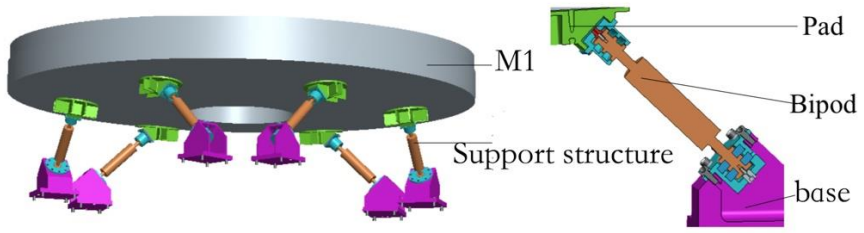

Figure 8. Three-dimensional model of the reflector assembly

The reflector constraint is subject to static and fixed constraint, and large additional assembly stress will not be introduced in the assembly process. The support structure has the characteristic of zero thermal deformation in axial direction within a certain range of temperature variation, which not only ensures the position accuracy of the reflector and the relative position precision of the primary and secondary mirrors in the orbit operation process of the satellite, but also ensures that the reflector assembly will not generate thermal stress due to temperature variation and thus have an impact on the surface accuracy of the reflector.

3.1. Design of the position parameters of the mirror supporting structure

The change of the spatial relative position of the Bipod bar and the reflector has certain influence on the basic frequency of the reflector component. Therefore, the spatial relative position of the Bipod bar and the reflector is optimized by taking the basic frequency of the reflector component as the target. The spatial relative position of the Bipod bar and the mirror is represented by two positional parameter variables, one of which is the Angle (α) between the projection of the Bipod bar on the back of the mirror and the radius of the mirror, as shown in figure 9.

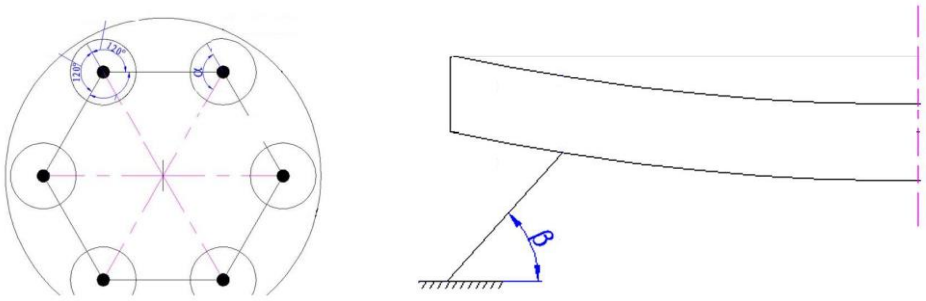

rojection diagram of Bipod bar on the back of the mirror(α)

Schematic diagram of the Angle between Bipod bar and main bearing plate (β)

Figure 9. The bipod bar Angle

The effect of the Angle between the projection of Bipod bar on the back of the mirror and the radius of the mirror on the base frequency of the reflector assembly is shown in table 7.

Table 7. influence of variation of Angle between Bipod bar and reflector radius on base frequency of reflector assembly

The Bipod bar is projected on the back of the mirror at an Angle to the radius /°	90	95	100	105	110	115
Basic frequency of reflector assembly /Hz	109.45	112.87	116.3	116.49	116.3	114.87

From the above data, the reflector components of fundamental frequency with the Bipod pole in the back of the mirror projection Angle and radius of reflector increases with the increase after the first decreases, and when the Angle is 100 ° ~ 110 ° between mirror component base frequency peak, considering the mirror supporting structure and the main bearing plate connection end interface design principles should be as far as possible compact, ultimately determine the Bipod rod in the back of the mirror projection and radius Angle is 100 °.

The other position parameter of the spatial relative position of the Bipod bar and the mirror is the Angle between the Bipod bar and the main bearing plate (β), as shown in figure 9.

The influence of the Angle between Bipod bar and main bearing plate on the base frequency of reflector assembly is shown in table 8.

Table 8 influence of variation of Angle between Bipod bar and main bearing plate on base frequency of reflector assembly

Angle between Bipod bar and main bearing plate /°	30	35	40	45	50
Basic frequency of reflector assembly /Hz	99.334	109.54	111.35	115.3	107.88

From the above data, the reflector components of fundamental frequency with the increase of the Bipod rod and main bearing plate Angle decreases after the first increases, when the Angle is 45 °

mirror component base frequency peak. The location parameters of the mirror support structure obtained from the final analysis are shown in table 9 below:

Table 9 optimal analysis results of mirror support structure position parameters

α /°	β /°
100	45

3.2. Mechanical analysis of reflector assembly structure and evaluation of profile accuracy

To ensure the accuracy of the reflector with excellent location and at a certain temperature conditions has good surface shape accuracy, this requires a reflector support structure has a certain stiffness on the one hand, to achieve mirror precise positioning, on the other hand support structure under the precondition of zero expansion characteristics of flexible, release the reflector due to temperature change of radial and axial thermal stress, to ensure that the mirror surface shape accuracy can meet the needs of camera imaging.

The satellite is in the state of zero gravity after entering the orbit, and the axial thermal deformation of the support structure along the Bipod bar is the main reason that affects the position accuracy and surface accuracy of the mirror[5]. Therefore, finite element software is used to optimize the design of the support structure, so that it has the characteristics of zero expansion along the axis of the Bipod bar. The finite element model of reflector component is shown in figure 10:

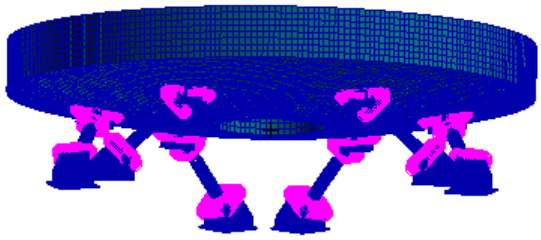

Figure 10. finite element model of reflector assembly

3.2.1. The modal analysis

The three translational degrees of freedom at the bottom of the constrained reflector component are calculated to obtain the first ten mode frequencies of the reflector component, among which the first five frequency modes are shown in table 10. The basic frequency of the reflector assembly is 106.9Hz.

Table 10. the five modal frequencies of the reflector assembly

No 1 106.9Hz	No 2 107.5 Hz	No 3 122.5 Hz
	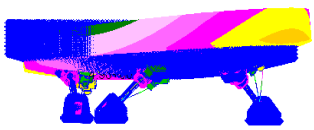	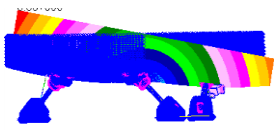
No 4 123.38 Hz	No 5 133.6 Hz	
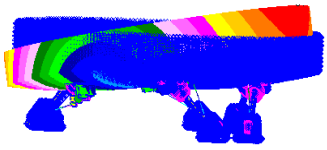		

3.2.2. Gravity impact analysis

1) X direction gravity impact analysis

The gravity acceleration of 1g along the X direction was applied to analyze the planar accuracy of the reflector assembly under the condition of six-point support. The stress cloud diagram and planar cloud diagram of the reflector assembly under the effect of gravity were shown in Figure. 11 below:

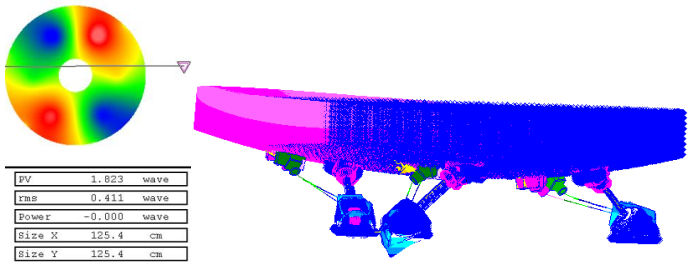

Figure 11. Reflection mirror component X - directional gravity deformation cloud diagram

The stress of each link of the reflector assembly under the effect of X gravity at 1g is shown in table 11 below:

Table 11 stress of mirror assembly under 1g gravity in Y direction

location	Mirror back adhesion	Glue spots	Titanium rod (flexible)	Aluminum cylinder	Invar cylinder	Potting cup
Stress value /MPa	0.219	0.101	9.23	0.869	0.532	4.63

2) Y direction gravity impact analysis

The gravity acceleration of 1g along the Y direction was applied to analyze the planar accuracy of the reflector assembly under the condition of six-point support. The stress cloud diagram and planar cloud diagram of the reflector assembly under the effect of gravity were shown in Figure. 12 below:

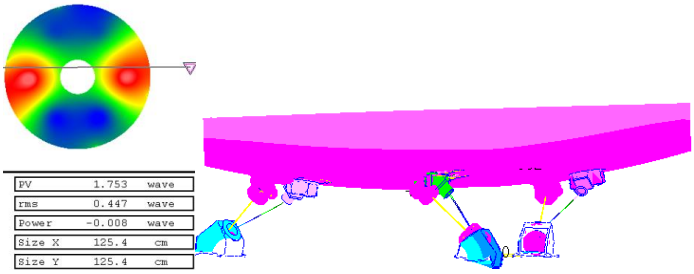

Figure 12 Reflection mirror component Y- directional gravity deformation cloud diagram

The stress of each link of the reflector assembly under the effect of Y gravity at 1g is shown in table 12 below:

Table 12 Stress of mirror assembly under the action of 1g gravity in Y direction

location	Mirror back adhesion	Glue spots	Titanium rod (flexible)	Aluminum cylinder	Invar cylinder	Potting cup
Stress value /MPa	0.163	0.1	8.75	0.897	0.49	4.51

3) Z direction gravity impact analysis

The gravity acceleration of 1g along the Z direction was applied to analyze the planar accuracy of the reflector assembly under the condition of six-point support. The stress cloud diagram and planar cloud diagram of the reflector assembly under the effect of gravity were shown in Figure. 13 below:

Figure 13 Reflection mirror component Z- directional gravity deformation cloud diagram

The stress of each link of the reflector assembly under the effect of Z gravity at 1g is shown in table 13 below:

Table 13. Stress of mirror assembly under the action of 1g gravity in Z direction

location	Mirror back adhesion	Glue spots	Titanium rod (flexible)	Aluminum cylinder	Invar cylinder	Potting cup
Stress value /MPa	0.094	0.06	2.99	0.54	0.28	2.7

3.2.3. Temperature load impact analysis

The finite-element method was used to analyze the profile accuracy and position accuracy of the reflector assembly under the conditions of uniform temperature variation, radial temperature gradient and axial temperature gradient.

1）Effect analysis of uniform temperature rise

Constraint reflector translational degree of freedom 6 base, put 1℃, homogeneous temperature changes reflecting mirror type changed accuracy 0.002 λ. The cloud picture of the reflector assembly under the condition of 1℃ temperature rise is shown in figure 14 below.

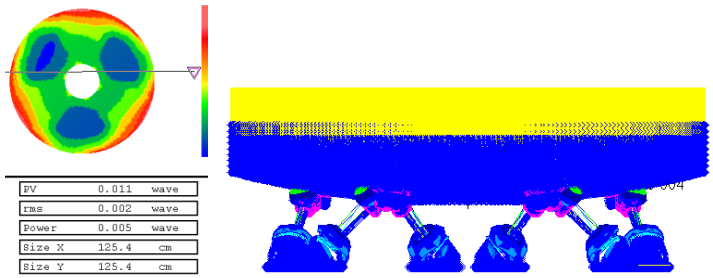

Figure. 14 deformation cloud diagram of reflector assembly with 1 degree temperature rise

Table 14 1℃ uniform temperature rise, the change of the optical axis

X translation	Y translation	Z translation	Rotation about X axis	Rotation about Y axis	Rotation about Z axis
0um	0um	0.651um	0''	0''	0''

2) impact analysis of radial temperature gradient change

When the reflector has a temperature gradient of 0.5 degree along the radial direction, the surface shape accuracy changes by 0.001 λ, and the surface shape cloud map under the temperature gradient is shown in figure 15.

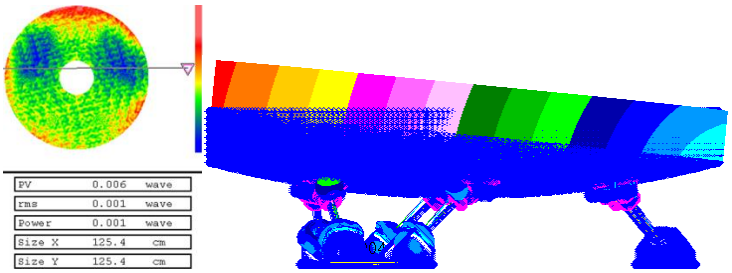

Figure 15. deformation cloud diagram of reflector assembly with radial 0.5 degree temperature gradient

Table 15 changes of optical axis with radial temperature gradient of 0.5 degree

X translation	Y translation	Z translation	Rotation about X axis	Rotation about Y axis	Rotation about Z axis
0um	0.1um	0.163um	0.05''	0''	0''

3) impact analysis of axial temperature gradient change

When there is a temperature gradient of 0.5 degree along the optical axis, the surface shape accuracy is reduced by 0.001 λ. The surface shape cloud map under the axial temperature gradient is shown in Figure. 16.

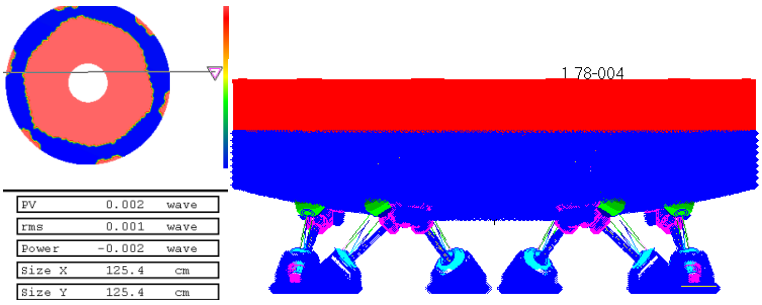

Figure 16. deformation cloud diagram of reflector assembly with axial 0.5 degree temperature gradient

Table 16. changes of optical axis with axial temperature gradient of 0.5 degree

X translation	Y translation	Z translation	Rotation about X axis	Rotation about Y axis	Rotation about Z axis
0um	0um	0.178um	0''	0''	0''

3.2.4. Forced displacement analysis of mirror assembly

The constrained reflector assembly has 5 bases, in which a forced displacement is applied to investigate the change of mirror RMS.

1) impact analysis of X-direction forced displacement:

The X-axis force displacement was 0.005mm, and the reflected mirror precision RMS changed by 0.002 λ. As shown in figure 17 below:

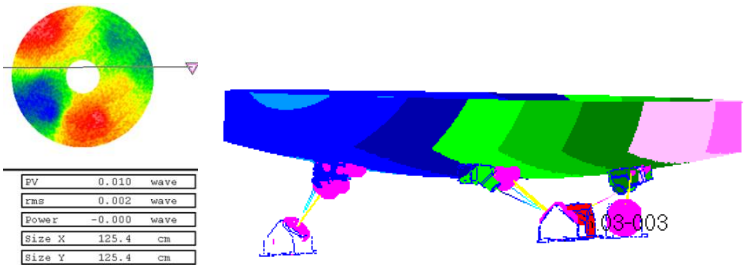

Figure 17. analysis of forced displacement in the X direction

Table 17. Axial change of the forced displacement mirror in X direction

X translation	Y translation	Z translation	Rotation about X axis	Rotation about Y axis	Rotation about Z axis
0.192um	1.261um	0.567um	0.4''	0.2''	0.4''

2) impact analysis of Y-direction forced displacement:

The forced displacement in the Y direction was 0.005mm. The reflected mirror precision RMS changed by 0.003 λ. As shown below:

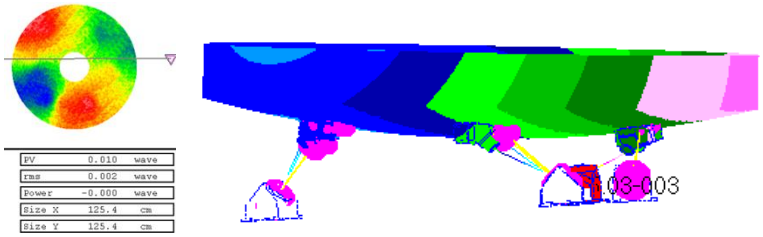

Figure18. analysis of forced displacement in the Y direction

Table 18. Axial change of the forced displacement mirror in Y direction

X translation	Y translation	Z translation	Rotation about X axis	Rotation about Y axis	Rotation about Z axis
0.198um	1.4725um	0.654um	0.4''	0.4''	0.4''

3) impact analysis of Z-direction forced displacement:

The z-direction forced displacement is 0.005mm. The reflected mirror precision RMS changes by 0.004 λ. As shown in figure 19 below:

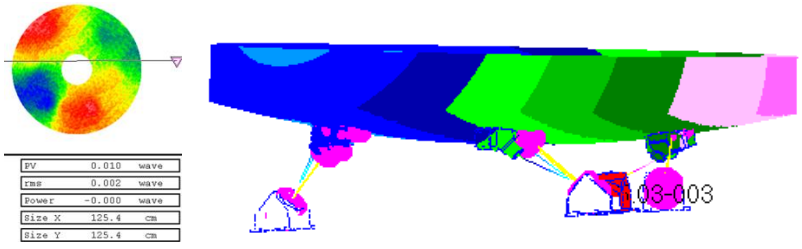

Figure 19. analysis of forced displacement in the Z direction

Table 19. Axial change of the forced displacement mirror in Z direction

X translation	Y translation	Z translation	Rotation about X axis	Rotation about Y axis	Rotation about Z axis
0.234um	1.834um	0.834um	0.6''	0.4''	0.6''

According to the above analysis results, the first natural frequency of the reflector assembly is 106.9Hz, which meets the dynamic stiffness requirements. Mirror component in 1 ℃ temperature, axial and radial temperature gradient, 0.005 mm condition under the action of assembly error, root mean square value of RMS is less than 0.004 λ surface shape change, translation is less than 2 um, meet the requirements of design index.

4. LIGHTWEIGHT REFLECTOR PROCESSING

1.3m-caliber reflectors have high light weight, small panel thickness and high difficulty in optical processing. The influence of processing pressure on mirror deformation is analyzed and calculated, processing steps and processing parameters are optimized, optimal processing removal function is selected at each stage, and strict correspondence between machining and detection data is achieved through nonlinear error correction method, so as to solve the problem of deterministic and quantitative processing in machining process.

The removal function of grinding and polishing process has an important influence on the convergence of the surface in optical processing. Therefore, it is necessary to simulate the removal function of grinding and polishing technology. Based on the mechanism of mechanical grinding removal and according to the Preston equation, the mathematical model of the horizontal rotating mechanical arm grinding and polishing numerical control is established. The motion speed of the robot relative to the optical disc can be obtained by the superposition principle of the vector as follows:

$$v(r)=\sqrt{v_1^2+v_2^2+2v_1v_2\cos\beta}=\sqrt{(r\omega_1)^2+(r\omega_2)^2+2r\omega_1r_1\omega_2\cos\beta} \tag{1}$$

Among them $\cos\beta=\dfrac{r^2+r_1^2-p_0^2}{2rr_1}$, $r_1=\sqrt{r^2+p_0^2-2rp_0\cos\theta}$

Assuming that the pressure and rotation speed of each point on the tool are consistent during the polishing process, the material removal amount is only related to the covering time of the tool working point. After theoretical simulation, the removal function of planetary motion can be obtained:

$$R(r)=CP\int_{-\theta_0}^{\theta_0}v(r)d\theta \tag{2}$$

According to the above formula, the computer simulation was carried out with matlab language and the normalization process was shown in figure 20. On this basis, the removal function was obtained through actual measurement.

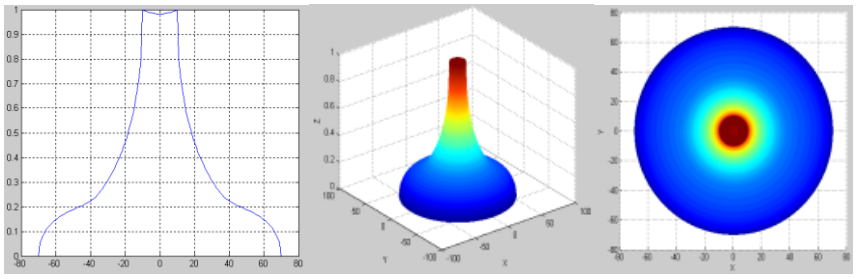

Figure 20. The normalized distribution of the function

In view of the characteristics of large initial surface shape low frequency error and large amount of removal, milling and grinding was first adopted, and the surface shape converges to 1 λ (RMS). After that, the surface shape converges to 0.014 λ (RMS) after a total of seven rounds of machining.

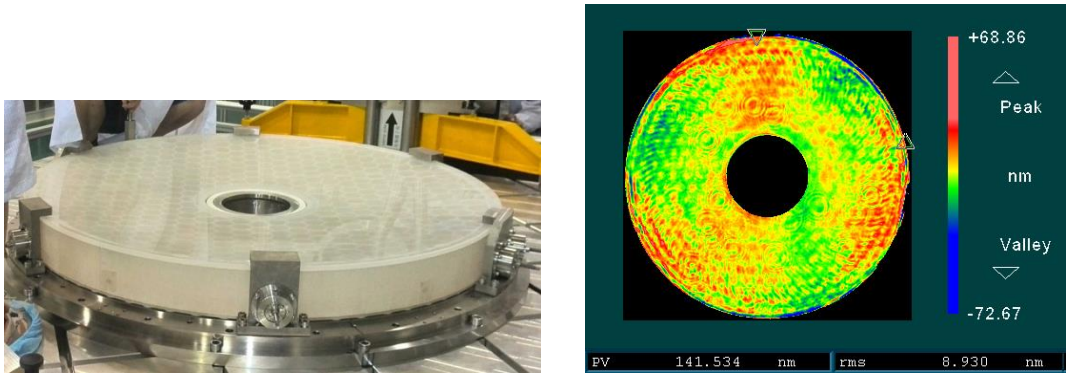

Reflector assembly before machining The precision of reflected mirror is greater than λ/70 RMS

Figure 21 Reflector processing

5. MIRROR ASSEMBLY AND BLENDING TEST

The primary task of the reflector assembly and tuning is to derive the reflector geometric datum. The mirror coordinate system is established with reflector as the reference point. Three points are distributed on the side of the mirror to test its coordinate value in the mirror coordinate system.

Invar pad uniform in the back of the mirror Φ 860 mm on the circumference of a circle of every 60 ° a total of six, and mirror on the back of the gap is 1 mm. A coordinate system is established for each Yin steel cushion with its center, underside (processed according to the plane) and pointed to the edge. The conversion relation between the coordinates of each invar cushion and the reflector coordinates was calculated.

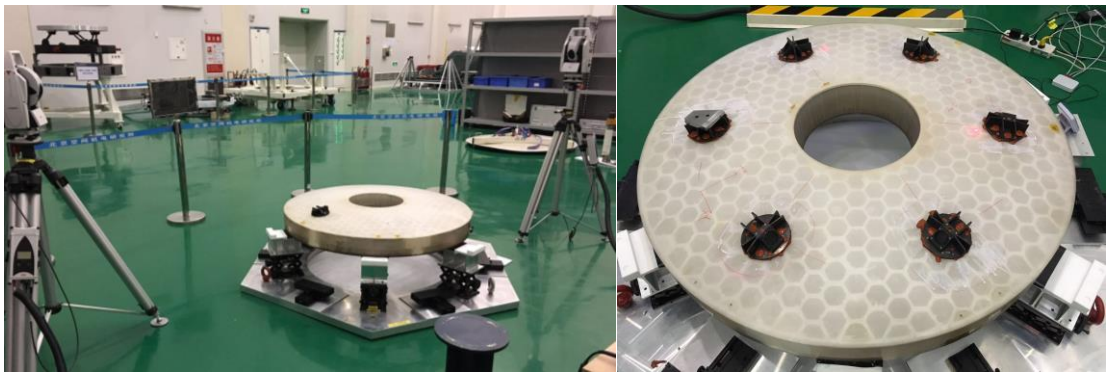

Figure 22. location of invar pad

According to the above coordinate values, adjust the position of each invar pad, and finally the deviation of each invar pad is within 0.15mm. On this basis, the installation of six Bipod bars was completed, and the reflector component profile was tested. Reflector around the mechanical axis rotation, every 60 ° to one direction, for a total of six direction in front of the form of a test.

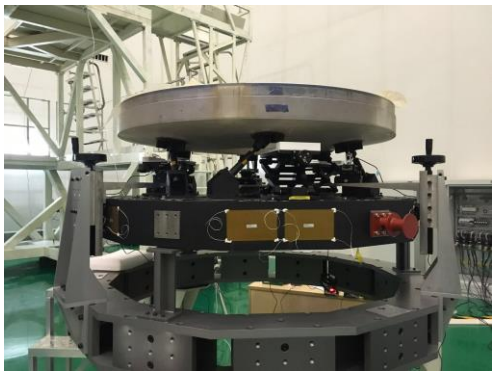

Figure 23 mirror component test

The average surface shape of the above 6 interference graphs was obtained by data processing using interferometer software. The result of measurement is almost the same as that of naked mirror.

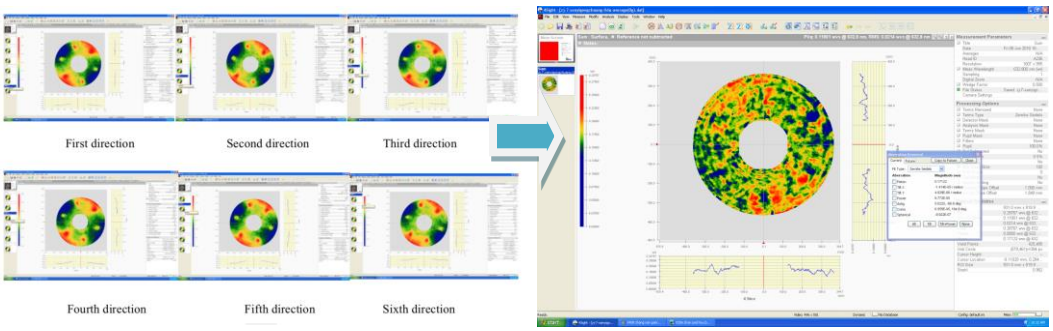

Figure 24. measurement and processing of profile data

6. CONCLUSION

According to the technical requirements of 1.3m caliber space mirror, detailed lens structure design and supporting structure design were carried out. Size according to the shape of the reflector, and the characteristics of the space application, selection of the arc back thick honeycomb sandwich structure, lightweight mirror is suitable for large caliber space mirror the Bipod support way, the entire positioning support structure light weight strong adaptability to environment, design the best position of strong point, finite element analysis of reflector components, in various conditions under the action of gravity, mirror surface shape accuracy meet the requirement of indicators, and suggests that mirrors can meet the requirements of space applications. By optimizing optical processing and assembling and adjusting process, the developed reflector components have been tested and reached the technical requirements. The experience of the reflector design can provide some reference for the same type of space reflector design.

REFERENCE LINKING

book: [1] Paul R. Yoder, Jr, [Opto-Mechanical Systems Design], Taylor & Francis Group

, 586-598 (2015).

journal paper: [2] Han Guangyu,Shao Shuai,Gao Yun-guo, et al.”The analysis&optimal for azimuthal support of primary mirror, ”Machinery Design&Manufacture, Vol.7,No.1,1001-3997(2009)

[3] Guomin Wang, Zhiyong Zhang, Bozhong Gu,et al.”Analysis and optimization of a 2.5m telescope mount,”Proc.SPIE 7018,,(2008)

[4] Songfeng Kou, Genrong Liu, Guomin Wang, “Optical system of Chinese SONG Telescope,” Proc. SPIE 8444,,(2012)

[5] M. R. Bolcar, K. Balasubramanian, M. Clampin, J. Crooke, L. Feinberg, M. Postman, M. Quijada, B. Rauscher, D. Redding, N. Rioux, et al., “Technology development for the advanced technology large aperture space telescope (atlast) as a candidate large uv-optical-infrared (luvoir) surveyor,” in SPIE Optical Engineering+ Applications, pp. 960209–960209, International Society for Optics and Photonics, 2015.

REFERENCES

[1] Paul R. Yoder, Jr, [Opto-Mechanical Systems Design], Taylor & Francis Group

, 586-598 (2015).

[2] Han Guangyu,Shao Shuai,Gao Yun-guo, et al.”The analysis&optimal for azimuthal support of primary mirror, ”Machinery Design&Manufacture, Vol.7,No.1,1001-3997(2009)

[3] Guomin Wang, Zhiyong Zhang, Bozhong Gu,et al.”Analysis and optimization of a 2.5m telescope mount,”Proc.SPIE 7018,,(2008)

[4] Songfeng Kou, Genrong Liu, Guomin Wang, “Optical system of Chinese SONG Telescope,” Proc. SPIE 8444,,(2012)

[5] M. R. Bolcar, K. Balasubramanian, M. Clampin, J. Crooke, L. Feinberg, M. Postman, M. Quijada, B. Rauscher, D. Redding, N. Rioux, et al., “Technology development for the advanced technology large aperture space telescope (atlast) as a candidate large uv-optical-infrared (luvoir) surveyor,” in SPIE Optical Engineering+ Applications, pp. 960209–960209, International Society for Optics and Photonics, 2015.